

Telomerase inhibition and cell growth arrest by G-quadruplex interactive agent in multiple myeloma

Masood A. Shammam,^{1,2,3} Robert J. Shmookler Reis,^{4,5} Masaharu Akiyama,^{1,2} Hemanta Koley,^{2,3} Dharminder Chauhan,^{1,2} Teru Hideshima,^{1,2} Raj K. Goyal,^{2,3} Laurence H. Hurley,⁶ Kenneth C. Anderson,^{1,2} and Nikhil C. Munshi^{1,2,3}

¹Boston VA Health Care System, West Roxbury, MA; ²Dana Farber Cancer Institute, Boston, MA; ³Harvard Medical School, Boston, MA; ⁴Departments of Geriatrics, and Biochemistry and Molecular Biology, University of Arkansas for Medical Sciences, Little Rock, AR; ⁵Central Arkansas Veterans Health Care System, Little Rock, AR; and ⁶Arizona Cancer Center and College of Pharmacy, University of Arizona, Tucson, AZ

Abstract

Objective: The aim of this study was to test the efficacy of telomerase inhibitor (TMPyP4 [tetra(*N*-methyl-4-pyridyl)-porphyrin chloride]; a G-quadruplex-intercalating porphyrin) as a potential therapeutic agent for multiple myeloma. **Materials and Methods:** We studied telomere length, telomerase activity, and effect of telomerase inhibition in multiple myeloma cells. Several myeloma cell lines were analyzed for telomerase activity, telomere length, and gene expression. Three myeloma cell lines (U266, ARH77, and ARD) were treated with TMPyP4 for 3–4 weeks. Viable cell number was assessed by trypan blue exclusion, and nature of cell death was determined by annexin labeling and/or DNA fragmentation. *In situ* oligo ligation technique was used to identify specific DNase I-type DNA cleavage. **Results:** We report high telomerase activity and shortened telomeres in myeloma cells compared to normal B cells. We have also observed inhibition of telomerase activity, reduction in telomere length, and decline of myeloma cell growth, as measured by trypan blue dye exclusion, following exposure to TMPyP4. Exposure to porphyrin reduced telomerase activity of U266, ARH77, and ARD myeloma cells by 98%, 92%, and 99%, respectively. Exposure to porphyrin had no effect on viability for the first 14 days, followed by death of 75–90% of cells over the next 2 weeks. The

nature of cell death was apoptotic, as determined by annexin and DNA nick labeling. Majority of cells showed DNA fragmentation specific to caspase-3-activated DNase I. **Conclusions:** These results demonstrate anti-proliferative activity of G-quadruplex-intercalating agents, and suggest telomerase as an important therapeutic target for myeloma therapy. (Mol Cancer Ther. 2003;2:825–833)

Introduction

In vertebrates, including humans, telomeric DNA is comprised of 500–3000 repeats of a conserved TTAGGG sequence (1–3). It is estimated that human telomeres lose 50–100 bp from their telomeric DNA at each mitosis (4). Telomere length therefore shortens progressively with each cell division, until the cell reaches an early crisis. Cells in early crisis have short (dysfunctional) telomeres, recognized as DNA damage and undergo p53-dependent apoptosis (5). In the absence of p53, continuous cell division results in severe telomere shortening and massive genetic instability (late crisis) (6).

Telomerase, a ribonucleoprotein with reverse transcriptase activity, adds G-rich repeats (TTAGGG) to the 3' end of telomeric DNA (7) and thereby overcomes an inherent limitation to proliferative capacity of a cell (8). Although germ-line cells and primitive hematopoietic cells express telomerase, it is below detectable limits in other somatic tissues (9). Transgenic expression of the telomerase protein in human diploid fibroblasts produces immortal clones (10), demonstrating that telomerase activity is required, although not necessarily sufficient, to extend replicative life span *in vitro*. Active telomerase, SV40 T antigen, and H-ras are jointly sufficient for sustained proliferation of human tumor cells in culture (11). Telomerase is reactivated in most cancers (12) and immortalized cell lines (12–14), due to somatic mutations or epigenetic changes (*e.g.*, demethylations).

On the other hand, telomerase-negative mice, although unimpaired initially (15), show hypoproliferative defects in susceptible organs by the sixth generation (16). Additional proliferation-related deficiencies appear during adult aging, including increased incidence of skin lesions, alopecia, graying hair, reduced body weight, atrophy of small intestinal cells, delayed healing, and diminished hematopoietic reserves (17).

Because telomerase activity is observed in most neoplastic cells and tissues, but is low or absent in noncancerous somatic cells (9, 12, 18), inhibitors of telomerase activity hold promise as anti-proliferative agents with specificity for tumor cells. Proliferative potential can be restricted in transformed cells by nucleic acids targeted to the telomerase RNA component. Transgenic expression of RNA complementary to telomerase RNA leads to shortened telomeres and reduced cell proliferation after an extended

Received 11/15/02; revised 2/3/03; accepted 6/20/03.

The costs of publication of this article were defrayed in part by the payment of page charges. This article must therefore be hereby marked advertisement in accordance with 18 U.S.C. Section 1734 solely to indicate this fact.

Grant support: Multiple Myeloma Research Foundation (2001 Fellow's Award) to M.A.S.; the Department of Veterans Affairs (Merit Review Award) to N.C.M.; and the Department of Veterans Affairs (Merit Review and REAP) to R.J.S.R.

Note: N.C.M. is a Leukemia Society Scholar in Translational Research.

Requests for reprints: Nikhil C. Munshi, Dana Farber Cancer Institute, 44 Binney Street M557, Boston, MA 02115. Fax: (617) 363-5592. E-mail: Nikhil_Munshi@DFCI.harvard.edu

lag phase (19, 20). Moreover, we have shown that treatment of immortal human cell lines with peptide nucleic acids complementary to telomerase RNA results in the loss of telomerase activity, telomere shortening, and reversal of immortality (21). Here we show that repeated treatment of myeloma cell lines with a G-quadruplex-intercalating telomerase inhibitor results in loss of telomerase activity, telomere shortening, and eventual apoptotic cell death. These results both extend our earlier observations and support the efficacy of telomerase inhibitors as potential anti-cancer agents.

Materials and Methods

Porphyryns

Tetramethyl (cationic) porphyryns have already been shown to inhibit telomerase activity in HeLa cell-free extracts and in intact MCF7 human breast carcinoma cells (22). TMPyP4 [tetra(*N*-methyl-4-pyridyl)-porphyrin chloride] is a porphyrin derivative able to intercalate in G-tetrad structures characteristic of telomeric DNA (22).

Cell Lines

Myeloma cell lines ARH77, 8226, U266, and HeLa were obtained from the American Type Culture Collection (Rockville, MD). Myeloma cell lines ARD, ARK, and ARP were kindly provided by Dr. J. Epstein, Myeloma and Transplantation Research Center at the Arkansas Cancer Research Center (ACRC). Primary cells were obtained as part of our approved clinical research protocol. Normal human diploid fibroblasts (GM01662) and ATSV1 cell line (Ataxia telangiectasia, GM05849) were obtained from the Genetic Mutant Cell Repository (National Institute for General Medical Sciences), maintained by the Coriell Institute for Medical Research, Camden, NJ. Myeloma cell lines were grown in RPMI 1640 supplemented with 10% fetal bovine serum, whereas diploid fibroblasts were cultured in DMEM with 10% fetal bovine serum, as described previously (21, 23).

Treatment and Growth of Cells

Constant numbers of cells were plated in multiple 100-mm dishes and treated with porphyryns at 1, 5, or 10 μ M, in a relatively dark room to reduce exposure of porphyryns to light. On day 7, the cells were harvested, counted, and replated at the same cell number per dish, with addition of the inhibitor at the same concentration. A portion of these cells ($1-2 \times 10^6$) was washed with PBS and stored at -70°C each week for assessment of telomerase activity and telomere length (see below).

Assay of Telomerase Activity

Telomerase activity was assayed using the TRAPeze Telomerase Detection Kit (Intergen, Purchase, NY) with products either visualized after gel electrophoresis or detected fluorometrically (TRAPeze XL kit). In the gel-electrophoresis protocol, porphyrin-treated cells were lysed and 1000 cell-equivalents of lysate were mixed with primer and TRAPeze reaction mixture. This reaction was incubated for 30 min at 30°C to allow telomerase-dependent elongation of "TS" primer. Elongated and amplified

telomerase products were resolved on 10% nondenaturing polyacrylamide gels. Intensities of internal standard and telomerase product bands were quantitated by Phosphor-Imager (Molecular Dynamics, Sunnyvale, CA), and telomerase activity (in TPG [total product generated] units) was calculated by comparing the ratio of telomerase products to an internal standard for each lysate, as described by Intergen. TPG is defined as the number of TS primers extended by at least four telomeric repeats through telomerase activity in an extract, during a 10-min incubation at 30°C . For fluorometric detection, lysates (1000 cell-equivalents) were mixed with TRAPeze XL reaction mix containing Amplifluor primers, and incubated for 30 min at 30°C . Elongated and amplified telomerase products were quantitated with a fluorescence plate reader (Spectra Max Gemini XS, Molecular Devices, Sunnyvale, CA).

Estimation of Telomere Length

Genomic DNA was isolated from cells using "Puregene" DNA isolation reagents (Gentra Systems, Minneapolis, MN) and telomere length was estimated as described previously (21). In brief, 6 μ g of genomic DNA was digested with a 6-fold excess of restriction enzyme *Hin*I (New England Biolabs, Beverly, MA), twice in succession. *Hin*I-digested DNA, along with a size standard (1 kb DNA ladder, Life Technologies, Inc., Gaithersburg, MD), was electrophoresed on 0.8% agarose gel and transferred to a nitrocellulose membrane as described previously (21). Membranes were then hybridized to ^{32}P -labeled (TTAGGG)₄ probe, and autoradiographic signal was scanned on a phosphorimager (Molecular Dynamics) with a 10^5 -fold linear response range. For each lane, the migration distance was determined for the median of the telomere restriction fragment distribution ("ImageQuant" software, Molecular Dynamics). Median (50th) and 90th percentile telomere length, in kbp, was then calculated by "Seqaid II" software (D. D. Rhoads and D. J. Roufa, Molecular Genetics Laboratory, Center for Basic Cancer Research, Kansas State University, Manhattan, KS 66506) using bands in the 1-kbp size marker as standards.

Apoptosis

Following 2–3 weeks of exposure to TMPyP4, apoptotic myeloma cells were detected by DNA fragmentation assay or by annexin V labeling. DNA fragmentation is based on nuclear labeling of recessed 3'-OH termini (Klenow FragEL, Oncogene Research Products, Boston, MA). The incorporation of peroxidase-labeled nucleotides is effected by Klenow DNA polymerase bound at free 3' ends of DNA cleaved by an endonuclease activated in apoptotic cells. Briefly, cells were plated and grown on Lab-Tek slides, and then fixed, rehydrated, permeabilized, and incubated with Klenow labeling mixture (containing Klenow enzyme, buffer, and biotinylated nucleotides). Nuclear labeling with biotinylated nucleotides was detected by subsequent incubation with streptavidin-horseradish peroxidase conjugate. Two hundred cells, representing at least five distinct microscopic fields, were counted to assess the fraction of labeled nuclei for each cell line.

For annexin V labeling, Annexin V-BIOTIN Apoptosis Detection Kit (Oncogene Research Products) was utilized. Briefly, 0.5 ml of cells (1×10^6 cells/ml) was mixed with annexin V-BIOTIN and incubated for 15 min at room temperature (RT). Cells were washed, resuspended in "Binding Buffer," and treated with streptavidin conjugated to FITC. Apoptotic cells were analyzed by a fluorescence microscope.

In Situ Oligo Ligation for Detection of Specific DNase I-Type Cleavage

Myeloma cells were treated with TMPyP4 for 3–4 weeks and apoptotic cells with specific DNase I-type cleavage were detected by ApopTag Peroxidase *In Situ* Oligo Ligation Kit (Intergen), as described by the manufacturer. Briefly, cells were fixed in methanol-free formaldehyde (1% in PBS; pH 7.4), dried, and postfixed in ethanol/acetic acid 2:1 (v/v). Fixed slides were incubated with a mixture of DNA ligase and a unique synthetic biotinylated oligo for 18 h at 16°C. After washing, the slides were sequentially treated with streptavidin-peroxidase, peroxidase substrate, mounted under a glass coverslip in mounting medium "permount," and viewed under a microscope.

Results

Telomerase Activity in Myeloma Cell Lines and Primary Myeloma Cells

We assayed telomerase activity in normal tonsillar plasma cells, normal diploid fibroblasts, and myeloma cells using the TRAPEze Telomerase Detection Kit (Intergen). The telomerase activity was extremely low at 0.004 TPG units for normal diploid fibroblasts and 0.01 units for normal plasma cells (Fig. 1). In contrast, telomerase activity was elevated 60- to 28,000-fold in myeloma cell lines, ranging from 0.6 TPG units in ARD cells to 280 TPG units in U266 cells. Telomerase activity in SV40-transformed fibroblasts (ATSV1) and in HeLa cells was 24 and 40 TPG units, respectively (Fig. 1).

Telomere Length in Myeloma Cell Lines

We next analyzed telomere length in six myeloma cell lines and normal plasma cells. "Telomere length," the mean size of telomeric restriction fragments generated by digesting the DNA with telomere-sparing restriction endonuclease *Hinf*I was estimated using genomic DNA isolated for each cell sample. The median (50th percentile) telomere length for normal plasma cells from three different normal donors was a mean of 7.3 ± 1.02 kbp (Fig. 2, lanes 1, 9, and 10). Telomere lengths in six myeloma cell lines (ARD, ARK, ARH, ARP, RPMI8226, and U266) ranged from 2.6 to 7.6 kbp, with a mean of 4.7 ± 1.2 kbp (Fig. 2, lanes 2–6 and 12). The median telomere length observed in the transformed fibroblasts—ATSV1 (Fig. 2, lane 11; see also Refs. 21, 24), was 2 kbp, approximately the putative minimum length for telomeres (4). Median telomere lengths in myeloma cell lines correlated inversely with telomerase activity (Spearman rank-order correlation coefficient r_s = linear correlation coefficient, $r = 0.8$, $P < 0.05$).

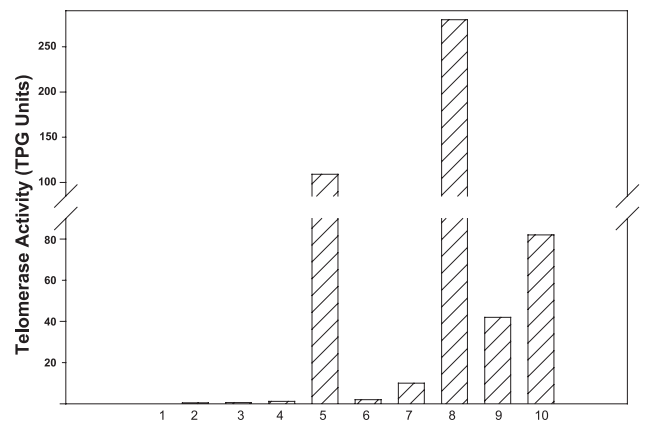


Figure 1. Assay of telomerase activity in myeloma cell lysates. Telomerase activity in cell lysates was determined using the TRAPEze Telomerase Detection Kit (Intergen). Cell lysate (1000 cell-equivalents) was mixed with a [32 P] end-labeled primer and TRAPEze reaction mixture, then incubated for 30 min at 30°C. Telomerase products were resolved on 10% nondenaturing polyacrylamide gels, which were dried and the autoradiographic signal scanned on a phosphorimager (Molecular Dynamics). Telomerase activity (in TPG units) was calculated by comparing the ratio of telomerase products to an internal standard for each lysate, as described by Oncor. Lanes, (1) lysis buffer; (2) diploid fibroblasts (GMO1662, negative control); (3) tonsillar plasma cells; (4) ARD; (5) U266; (6) ARP; (7) 8226; (8) U266; (9) ATSV1 transformed fibroblasts; (10) HeLa cells.

Inhibition of Telomerase Activity in Myeloma Cells by Porphyrins

TMPyP4, a porphyrin derivative that intercalates in G-quadruplex DNA, effectively inhibits telomerase activity *in vitro* (22). We tested its effects on human myeloma cell lines with medium, short, and long telomeres. Myeloma cell lines U266 (median TL; 4.0 kbp), ARH (median TL; 2.7 kbp), and ARD (median TL; 7.6 kbp) were treated with TMPyP4 at 1, 5, or 10 μ M for 7 days, harvested, and assessed for telomerase activity. Telomerase activity was inhibited by $\geq 90\%$ in all three cell lines by 10 μ M TMPyP4 (Fig. 3). A similar inhibition was induced by 5 μ M TMPyP4 in ARH77 cells (Fig. 3B, lane 3) and 1 μ M TMPyP4 in ARD cells, which have the lowest level of telomerase activity (Fig. 3C, lane 1).

To study the time course of telomerase inhibition, myeloma cells (U266) were treated with the most effective dose of TMPyP4 (10 μ M) for 1, 3, 5, and 7 days, and evaluated for telomerase activity. As shown in Fig. 3D, telomerase activity was reduced by 23% on day 1 (lane 2), by 50% on day 3 (lane 3), and almost completely on days 5 and 7 (lanes 4 and 5).

Growth Inhibition following Porphyrin Treatment of Human Cells

U266, ARH77, and ARD myeloma cell lines were treated with TMPyP4 at the minimal concentration which blocked $>90\%$ of telomerase activity, and viability assessed weekly by trypan blue exclusion. A marked arrest of cell proliferation was observed in all three cell lines (Fig. 4). Viable cell number remained stable for the first 2 weeks,

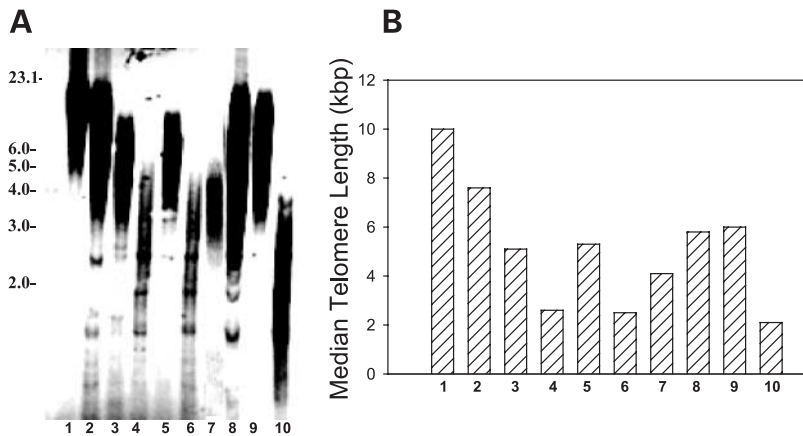


Figure 2. Telomere length of DNA isolated from myeloma cell lines and primary cultures. **A**, genomic DNA (6 μ g) was digested twice with a 6-fold excess of *Hinf*I endonuclease, electrophoresed on 0.8% agarose gel, and transferred to a nitrocellulose membrane as previously described 21. Membranes were then hybridized to a 32 P-labeled (TTAGGG)₄ probe and the autoradiographic signal was scanned. **Lanes** are as described below. **B**, median telomere fragment lengths, calculated from size distributions in scanned lanes. **Lanes**, (1) normal plasma cells from tonsils; (2) ARD; (3) ARK; (4) ARH77; (5) ARP; (6) 8226; (7) U266; (8) normal plasma cells, donor 1; (9) normal plasma cells, donor 2; (10) ATSV1.

and then declined by 75–84% over the next 2 weeks. Treatment with TMPyP4 induced $78 \pm 3\%$ cell death in U266 cells, $77 \pm 4\%$ cell death in ARH77 cells, and $84 \pm 4\%$ cell death in ARD cells (Fig. 4, A–C).

We also monitored the effect of a shorter exposure to TMPyP4 on continued growth of myeloma cells in culture. Myeloma cells U266 and ARD were treated with 10 and 1 μ M TMPyP4, respectively, for 5 days. The cells were washed with PBS three times, and incubated in fresh TMPyP4-free medium, and viability assessed weekly by trypan blue exclusion. As seen in Fig. 4, an initial 5-day exposure of U266 (Fig. 4D) and ARD (Fig. 4E) myeloma cells to TMPyP4, followed by re-incubation in porphyrin-free medium did not result in growth arrest of these cells, even at week 5.

Effect of Telomerase Inhibitors on Telomere Length

Median (50th percentile) and 90th percentile telomere lengths were determined in U266, ARH, and ARD myeloma cells after treatment with porphyrin. Median telomere length in U266 cells was reduced by 800 bp (*i.e.*, by 20% of the initial median value; Fig. 5, A and E) in 4 weeks. TMPyP4 reduced median telomere length by 340 bp (*i.e.*, by 5.1% of the initial median value) in ARD cells (Fig. 5, C and E) and by 90 bp (by 4.3% of the initial median) in ARH77 cells (Fig. 5, B and E). TMPyP4 exerted its greatest effect on the longest telomeres, reducing the 90th percentile size by 900 bp (22%) in U266 (Fig. 5D), 7.8 kbp (41%) in ARD (Fig. 5D), and by 460 bp (11%) in ARH77 cells (Fig. 5D).

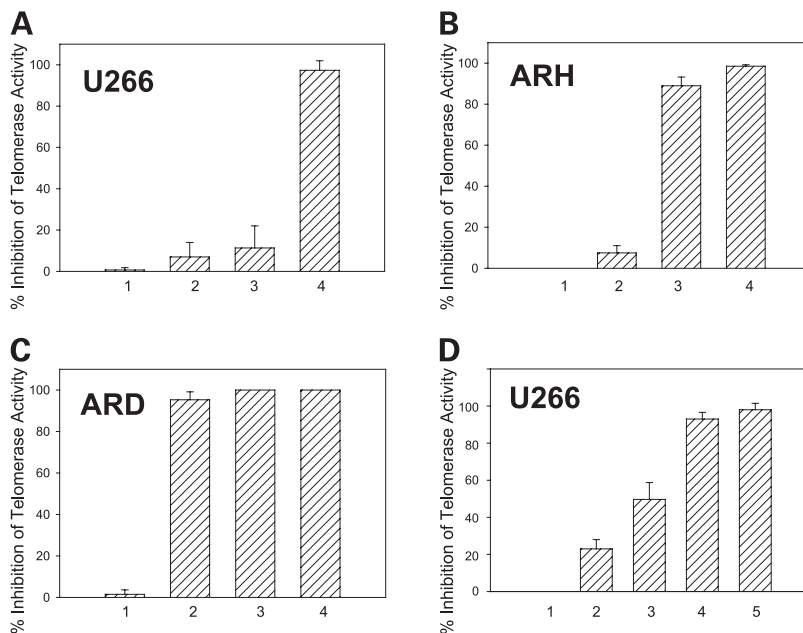
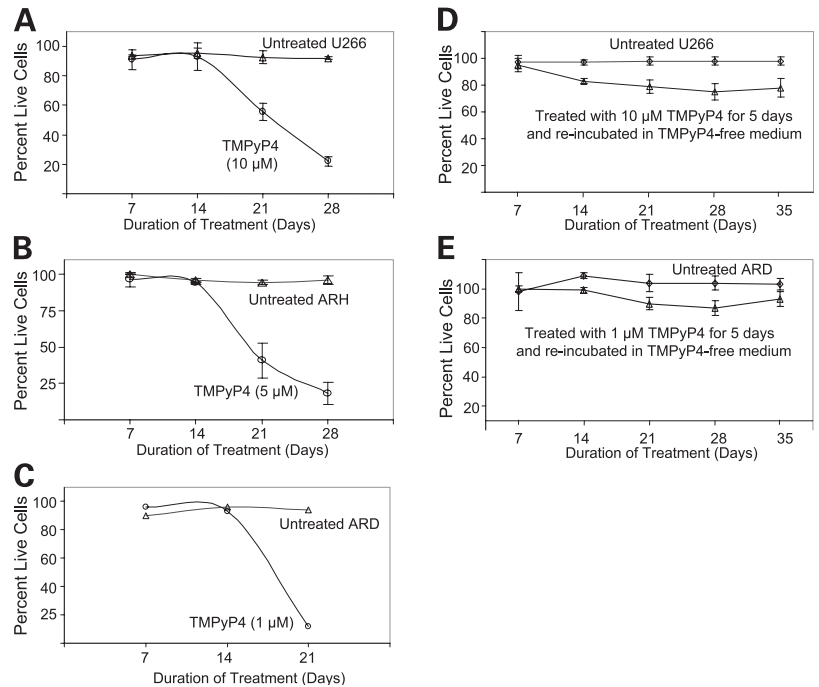


Figure 3. Assay of telomerase activity in lysates of porphyrin-treated myeloma cells. Telomerase activity in porphyrin-treated cells was determined using the TRAPeze XL Telomerase Detection Kit (Intergen). Lysate (1000 cell-equivalents) was mixed with TRAPeze XL reaction mix containing Amplifluor primers, and incubated for 30 min at 30°C. Telomerase products were amplified and quantitated using a fluorescence plate reader. **A**, percentage inhibition of telomerase activity in porphyrin-treated U266 cells relative to untreated control is shown. **Lanes**, (1) untreated U266 cells, (2) U266 cells treated with 1 μ M TMPyP4 for 7 days, (3) U266 cells treated with 5 μ M TMPyP4 for 7 days, (4) U266 cells treated with 10 μ M TMPyP4 for 7 days. **B**, percentage inhibition of telomerase activity in porphyrin-treated ARH cells relative to untreated control is shown. **Lanes**, (1) untreated ARH77 cells, (2) ARH77 cells treated with 1 μ M TMPyP4 for 7 days, (3) ARH77 cells treated with 5 μ M TMPyP4 for 7 days, (4) ARH77 cells treated with 10 μ M TMPyP4 for 7 days. **C**, percentage inhibition of telomerase activity in porphyrin-treated ARD cells relative to untreated control is shown. **Lanes**, (1) untreated ARD, (2) ARD cells treated with 1 μ M TMPyP4 for 7 days, (3) ARD cells treated with 5 μ M TMPyP4 for 7 days, (4) ARD cells treated with 10 μ M TMPyP4 for 7 days. **D**, percentage inhibition of telomerase activity in porphyrin-treated U266 cells relative to untreated control. **Lanes**, (1) untreated, (2) treated for 1 day, (3) treated for 3 days, (4) treated for 5 days, (5) treated for 7 days.

Figure 4. Limited replicative potential of myeloma cells treated with porphyrins. **A**, growth curve for U266 cells. Cells were grown 7 days in medium containing no porphyrin (*triangles*) or 10 μM TMPyP4 (*circles*). At the end of each 7-day treatment cycle, cells were harvested and the number of viable (trypan blue excluding) cells was counted. **B**, growth curve for ARH77 cells. Cells were grown 7 days in medium containing no porphyrin (*triangles*), or 5 μM TMPyP4 (*circles*). At the end of each 7-day treatment cycle, cells were harvested and the number of viable (trypan blue excluding) cells was counted. **C**, growth curve for ARD cells. Cells were grown 7 days in medium containing no porphyrin (*triangles*), or 1 μM TMPyP4 (*circles*). At the end of each 7-day treatment cycle, cells were harvested and the number of viable (trypan blue excluding) cells was counted. Results from two independent experiments. **D**, U266 cells were grown in the presence of 10 μM TMPyP4 for 5 days and re-incubated in drug-free medium. Viable (trypan blue excluding) cell number was counted weekly. **E**, ARD cells were grown in the presence of 1 μM TMPyP4 for 5 days and re-incubated in drug-free medium. Viable (trypan blue excluding) cell number was counted weekly.

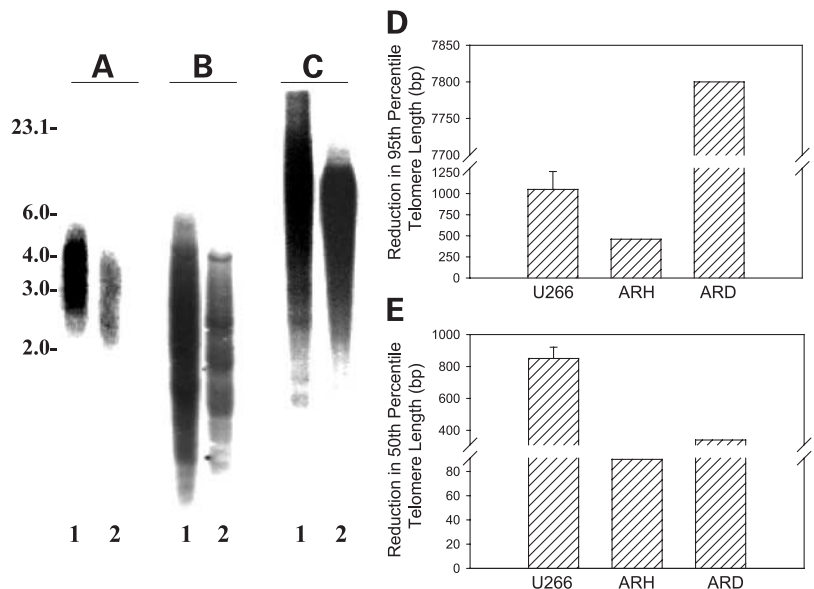


The Nature of Cell Death following Telomerase Inhibition

We utilized annexin V labeling and DNA fragmentation to assess apoptosis, at the start of growth arrest. As shown in Fig. 6, >70% annexin V-labeled U266 cells were observed following a 3-week treatment with TMPyP4 (Fig. 6, D and E) *versus* 18% untreated U266 cells, indicating a significant difference ($P < 0.05$) (Fig. 6, B and E). Similarly, ~12% ARH77 cells and 45% ARD cells appeared apoptotic after 3 and 2 weeks of treatment with TMPyP4, compared to 0% and 8% apoptotic cells for untreated ARH and ARD lines, respectively (Fig. 6, F and G).

To indicate the apoptotic pathway, we identified specific DNase I-type cleavages in myeloma cells treated for 3–4 weeks with TMPyP4, utilizing ApopTag Peroxidase *In Situ* Oligo Ligation Kit (Intergen). Briefly, cells were fixed and incubated with a mixture of DNA ligase and a unique synthetic biotinylated oligo. Because of the specificity of T4 DNA ligase and unique design of synthetic oligo, it would specifically ligate genomic DNA carrying DNase I-type cleavage. The ligation complexes were identified by sequential treatments with streptavidin-peroxidase, and peroxidase substrate, and visualized under a microscope.

Figure 5. Reduction in telomere length following porphyrin treatment of myeloma cells. U266, ARH77, and ARD cells were treated with porphyrins, as indicated. Telomere terminal restriction fragments were measured as described. **A**, DNA was analyzed from U266 cells that were (1) untreated or (2) treated with 10 μM porphyrin TMPyP4 for 28 days. **B**, DNA was analyzed from ARH77 cells that were (1) untreated or (2) treated with 5 μM porphyrin TMPyP4 for 28 days. **C**, DNA was analyzed from ARD cells that were (1) untreated or (2) treated with 1 μM active porphyrin TMPyP4 for 21 days. **D**, telomeric DNA restriction fragments, 90th percentile lengths, calculated from U266, ARH77, and ARD telomere fragment size distributions in scanned lanes as in **A**, **B**, and **C** in the figure. **E**, telomeric DNA restriction fragments, 50th percentile lengths (median), calculated from U266, ARH77, and ARD telomere fragment size distributions in scanned lanes as in **A**, **B**, and **C** in the figure.



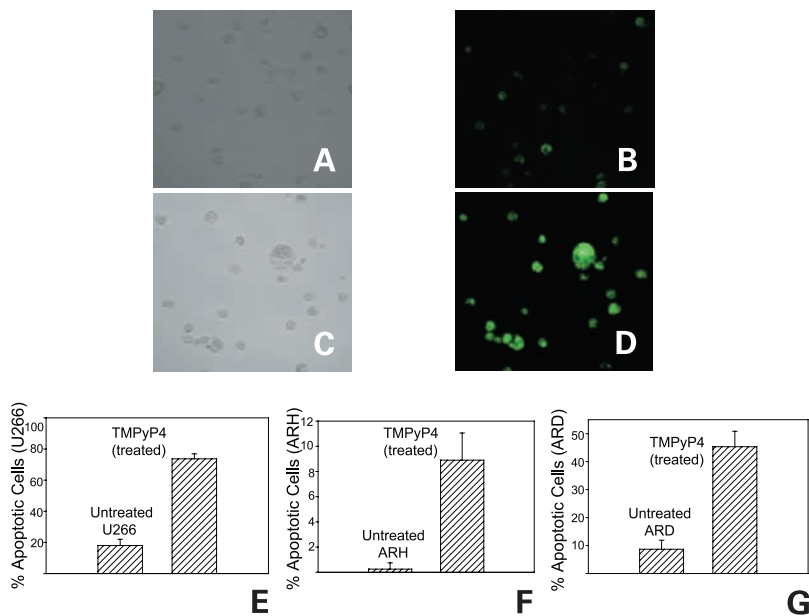


Figure 6. Apoptosis following porphyrin treatment of myeloma cells. U266 cells, untreated and treated with 10 μM TMPyP4 for 21 days, were analyzed for apoptosis utilizing Annexin V-BIOTIN Apoptosis Detection Kit (Oncogene Research Products). Briefly, cells were mixed with annexin V-BIOTIN, incubated for 15 min at room temperature and treated with streptavidin conjugated to FITC. Apoptotic cells were photographed and viewed by phase contrast and by fluorescence emitted at 518 nm. **A**, untreated U266 cells, viewed by phase contrast. **B**, untreated U266 cells, viewed by fluorescence. **C**, TMPyP4-treated U266 cells, viewed by phase contrast. **D**, TMPyP4-treated U266 cells, viewed by fluorescence. **E**, percentage apoptotic U266 cells, determined by examining ~200 cells representing five different microscopic fields. **F**, ARH77 cells were treated for 21 days with 5 μM porphyrin TMPyP4 and then examined for apoptosis by a DNA fragmentation assay (Klenow FragEL). **G**, ARD cells treated for 14 days with 1 μM TMPyP4 and then examined for apoptosis by a DNA fragmentation assay (Klenow FragEL).

As seen in Fig. 7, nuclei of the cells with DNase I-type cleavage are labeled dark brown. Myeloma cell lines U266 (Fig. 7A), ARH (Fig. 7B), and ARD (Fig. 7C) treated with TMPyP4 showed 62%, 71%, and 68% cells with DNase I-type cleavage, respectively. Because DNase I is activated by caspase-3, both of these enzymes may play a major role in TMPyP4-induced apoptosis.

Discussion

Maintenance of telomere length is critical for continued growth and survival of tumor cells, and telomerase activation maintains telomeres in proliferating tumor cells. In this study, we observed a high level of telomerase

activity in all myeloma cell lines tested, *versus* low-level telomerase activity in normal diploid fibroblasts and normal plasma cells. There was an inverse correlation ($r = r_s = -0.8$) between telomere length and telomerase activity among myeloma cell lines, as previously reported in B-cell chronic lymphocytic leukemia (25). These findings are also consistent with observations in non-hematopoietic cancers such as hepatocellular carcinoma (26), breast cancer (27), and prostate cancer (28), in which shortened telomeres are associated with elevated telomerase activity. In our study, telomeres were shorter in myeloma than in normal plasma cells, suggesting that telomerase directed therapy may induce crisis after fewer cell divisions.

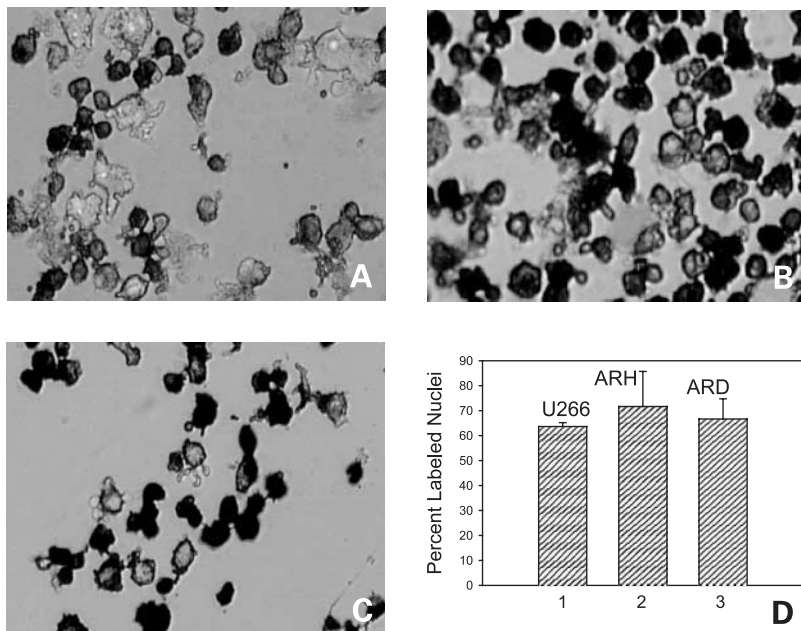


Figure 7. Identification of specific DNase I-type cleavages in TMPyP4-treated myeloma cells. Cells were fixed and incubated with a mixture of DNA ligase and a unique synthetic biotinylated oligo. The ligation complexes were identified by sequential treatments with streptavidin-peroxidase, and peroxidase substrate, and visualized under microscope. **A**, U266 cells treated with 10 μM TMPyP4 for 28 days. **B**, ARH cells treated with 5 μM TMPyP4 for 28 days. **C**, ARD cells treated with 1 μM TMPyP4 for 21 days. **D**, percentage labeled nuclei, indicative of specific DNase I-type DNA ends.

In the present study, we assessed telomerase activity and telomere length in a panel of myeloma cell lines, and selected three myeloma lines representing the spectrum of telomerase activity and telomere length. These lines (U266, ARH77, and ARD) were then treated with G-quadruplex-intercalating cationic porphyrin and tested for inhibition of telomerase activity and cell proliferation. Such tetramethyl porphyrins localize preferentially in nuclei, where they can bind and stabilize the G-quadruplex structures including telomeric DNA (22). A number of cationic porphyrins have been shown to inhibit telomerase in normal and tumor cell lines including HeLa and MCF7 (22) at subcytotoxic concentrations. In our study, TMPyP4 (1 μM) inhibited telomerase activity in ARD cells, whereas $\geq 5 \mu\text{M}$ TMPyP4 were needed to inhibit 90% of telomerase activity in U266 and ARH77 cells, both with higher telomerase levels. Reduction in telomerase activity was detectable as early as 24 h following treatment, although it required 5 days to observe complete inhibition of telomerase activity *in vivo* (Fig. 3D). Unlike MiaPaCa-2 (human pancreatic tumor) cells (29), human myeloma cells showed no change in transcript or protein levels of telomerase reverse transcriptase (hTERT) following exposure to TMPyP4.¹

Importantly, we observed that continuous presence of TMPyP4 is associated with a marked arrest of myeloma cell proliferation. Cell death following treatment with porphyrins occurred after a lag period of 2–4 weeks, suggesting a requirement to reach a critical telomere length threshold, which induces growth arrest and apoptosis. Consistent with this, porphyrin-mediated growth arrest of myeloma cells was also associated with reduction in telomere length. Telomere shortening was more pronounced at the high end of their size range (the 90th percentile) than at the median length. For continued cell proliferation, cellular selection favoring lineages that display either reactivated telomerase, or increased recombination supporting both mutation (activating oncogenes and inactivating antioncogenes) and telomere expansion by intertelomere exchange, is required (30, 31). In such a scenario, critically short telomeres at any one chromosome end may limit cell replication, preventing further shortening of already minimal-length telomeres, while allowing reduction in the longest telomeric fragments (90th percentile) as we observed in ARH77 and ARD cells. The abrupt, >9-fold increase in cell death observed after a prolonged lag phase suggests gradual telomere shortening followed by a critical telomere length threshold leading to apoptosis, which we confirmed using annexin V staining and DNA fragmentation assay. We have previously reported that introduction of peptide nucleic acid (PNA) oligonucleotides complementary to the RNA component of telomerase into transformed human fibroblasts inhibited

telomerase activity, shortened median telomere length, and after a lag period of 2 weeks gradually reduced the proliferative potential, leading to reversal of their immortality (21), a response kinetic similar to the present study.

To identify the major pathway involved in TMPyP4-mediated apoptosis, we have utilized “*In Situ* Oligo Ligation (ISOL) technique” which specifically labels DNase I-type cleavage and does not recognize single-stranded DNA, 3'-recessed ends, 3'-overhanging ends longer than one (dT) base, nicks, or gaps. Apoptosis-specific DNases are activated either by serine proteases or caspases (32). DNase I belongs to apoptosis-specific “Ca²⁺- and Mg²⁺-dependent endonucleases,” which in normal cellular environment is inhibited by poly(ADP-ribose)ation. Caspase-3-mediated cleavage of poly(ADP-ribose) polymerase (PARP) and actin (33, 34) activates DNase I which is responsible for specific DNA cleavage. Because majority of cells in all three cell lines showed DNase I-type cleavage, caspase-3-mediated activation of DNase I seems to be the major pathway of apoptosis following exposure to TMPyP4.

In an effort to identify apoptotic pathway and initiator caspase/s following exposure of myeloma cells to TMPyP4, we have evaluated gene expression profile of the key proteins involved in apoptosis following 2 weeks of exposure of MM1S myeloma cells to TMPyP4 (data not shown). We observed marked down-regulation of the transcript levels of mitochondrion-dependent apoptosis-related genes, including death effector filament-forming Ced-4-like apoptosis protein, caspase recruitment domain protein 10, and apoptotic protease activating factor (APAF) (35), which were down-regulated 1.6-, 7.4-, and 106-fold, respectively, in TMPyP4-treated cells. Caspase-9, which is the initiator of mitochondrion-dependent apoptosis pathway, was not detected; whereas transcript levels of genes involved in death receptor-dependent apoptosis pathway were detected and/or up-regulated. These include CASP8- and FADD-like apoptosis regulator (CASP8/CASPER/CLARP), caspase-10 (36, 37), and caspase-1, an interleukin-1 processing enzyme (38) also implicated in death receptor-dependent apoptosis (39, 40). Among effector caspases, caspase-3 was detected and caspase-6 was >2-fold up-regulated. Together these data suggest that exposure to TMPyP4 initiates death receptor-dependent apoptosis pathway through overexpression of CASP8/CASPER, which is then executed by caspase-3, caspase-6, and DNase I. These data provide basis for further evaluation of terminal signaling that may be activated following telomere shortening and may allow us to explore combinations of agents that may have synergistic activity along with TMPyP4.

As TMPyP4 binds to both intra- and intermolecular G-quadruplex structures, it may also alter cellular transcriptional activity leading to cell death by mechanisms other than telomerase inhibition. We have compared gene expression profile following exposure of myeloma cells to TMPyP4 (an inter- or intramolecular G-quadruplex intercalator), and RNAi against hTERT (specific telomerase inhibitor) at days 1 and 7 following treatment. Most genes related to apoptosis and cell cycle

¹ M. A. Shamma, R. J. Schmoockler Reis, C. Li, H. Koley, K. C. Anderson, and N. C. Munshi. Gene expression profile of multiple myeloma cells following treatment with telomerase inhibitors, submitted for publication.

control remained unaffected following exposure to the drug, suggesting lack of effect of this agent on other cellular transcriptional activity at the concentrations used. This information along with the prolonged exposure required to induce cell death and reduction of telomere length associated with TMPyP4 exposure suggest that effects were predominantly due to its action on telomerase activity (22).

Our study therefore shows that myeloma cell lines have relatively short telomeres and elevated telomerase activities, typical of many tumor cell types. As in several other cancers and immortal cell lines examined previously including breast carcinoma (41), Burkitt lymphoma (41, 42), immortal human breast epithelial cells (43), and SV40-immortalized fibroblast lines ATSV1, ATSV2, and CYS-SV (21), myeloma cells undergo growth arrest and apoptosis after prolonged inhibition of telomerase activity. Ongoing studies are evaluating more active and specific inhibitors as well as delineating apoptotic pathways induced by these agents to validate telomerase as a novel therapeutic target in myeloma and provide the framework for clinical trials of inhibitors, alone or combined with conventional and other novel therapies to improve patient outcome in myeloma.

References

- Allshire, R. C., Gosden, J. R., Cross, S. H., Cranston, G., Rout, D., Sugawara, N., Szostak, J. W., Fantes, P. A., and Hastie, N. D. Telomeric repeat from *T. thermophila* cross hybridizes with human telomeres. *Nature*, **332**: 656–659, 1988.
- de Lange, T., Shiu, L., Myers, R. M., Cox, D. R., Naylor, S. L., Killery, A. M., and Varmus, H. E. Structure and variability of human chromosome ends. *Mol. Cell Biol.*, **10**: 518–527, 1990.
- Moyzis, R. K., Buckingham, J. M., Cram, L. S., Dani, M., Deaven, L. L., Jones, M. D., Meyne, J., Ratliff, R. L., and Wu, J. R. A highly conserved repetitive DNA sequence, (TTAGGG)*n*, present at the telomeres of human chromosomes. *Proc. Natl. Acad. Sci. USA*, **85**: 6622–6626, 1988.
- Harley, C. B., Futcher, A. B., and Greider, C. W. Telomeres shorten during ageing of human fibroblasts. *Nature*, **345**: 458–460, 1990.
- Hayflick, L. The cellular basis for biological aging. In: C. E. Finch and Hayflick, L. (eds.), *Handbook of the Biology of Aging*, pp. 159–186. NY: Van Nostrand Reinhold Co., 1977.
- Chin, L., Artandi, S. E., Shen, Q., Tam, A., Lee, S. L., Gottlieb, G. J., Greider, C. W., and DePinho, R. A. p53 deficiency rescues the adverse effects of telomere loss and cooperates with telomere dysfunction to accelerate carcinogenesis. *Cell*, **97**: 527–538, 1999.
- Blackburn, E. H. Telomerases. *Annu. Rev. Biochem.*, **61**: 113–129, 1992.
- Engelhardt, M., Kumar, R., Albanell, J., Pettengell, R., Han, W., and Moore, M. A. Telomerase regulation, cell cycle, and telomere stability in primitive hematopoietic cells. *Blood*, **90**: 182–193, 1997.
- Kim, N. W., Piatyszek, M. A., Prowse, K. R., Harley, C. B., West, M. D., Ho, P. L., Coviello, G. M., Wright, W. E., Weinrich, S. L., and Shay, J. W. Specific association of human telomerase activity with immortal cells and cancer [see comments]. *Science*, **266**: 2011–2015, 1994.
- Bodnar, A. G., Ouellette, M., Frolkis, M., Holt, S. E., Chiu, C. P., Morin, G. B., Harley, C. B., Shay, J. W., Lichtsteiner, S., and Wright, W. E. Extension of life-span by introduction of telomerase into normal human cells [see comments]. *Science*, **279**: 349–352, 1998.
- Hahn, W. C., Counter, C. M., Lundberg, A. S., Beijersbergen, R. L., Brooks, M. W., and Weinberg, R. A. Creation of human tumour cells with defined genetic elements [see comments]. *Nature*, **400**: 464–468, 1999.
- Shay, J. W. and Bacchetti, S. A survey of telomerase activity in human cancer. *Eur. J. Cancer*, **33**: 787–791, 1997.
- Avilion, A. A., Piatyszek, M. A., Gupta, J., Shay, J. W., Bacchetti, S., and Greider, C. W. Human telomerase RNA and telomerase activity in immortal cell lines and tumor tissues. *Cancer Res.*, **56**: 645–650, 1996.
- Shay, J. W. and Wright, W. E. The reactivation of telomerase activity in cancer progression. *Trends Genet.*, **12**: 129–131, 1996.
- Blasco, M. A., Lee, H. W., Hande, M. P., Samper, E., Lansdorp, P. M., DePinho, R. A., and Greider, C. W. Telomere shortening and tumor formation by mouse cells lacking telomerase RNA [see comments]. *Cell*, **91**: 25–34, 1997.
- Lee, H. W., Blasco, M. A., Gottlieb, G. J., Horner, J. W., 2nd, Greider, C. W., and DePinho, R. A. Essential role of mouse telomerase in highly proliferative organs. *Nature*, **392**: 569–574, 1998.
- Rudolph, K. L., Chang, S., Lee, H. W., Blasco, M., Gottlieb, G. J., Greider, C., and DePinho, R. A. Longevity, stress response, and cancer in aging telomerase-deficient mice. *Cell*, **96**: 701–712, 1999.
- Broccoli, D., Young, J. W., and de Lange, T. Telomerase activity in normal and malignant hematopoietic cells. *Proc. Natl. Acad. Sci. USA*, **92**: 9082–9086, 1995.
- Feng, J., Funk, W. D., Wang, S. S., Weinrich, S. L., Avilion, A. A., Chiu, C. P., Adams, R. R., Chang, E., Allsopp, R. C., Yu, J., Le, S., West, M. D., Harley, C. B., Andrews, W. H., Greider, C. W., and Villeponteau, B. The RNA component of human telomerase. *Science*, **269**: 1236–1241, 1995.
- Kondo, S., Tanaka, Y., Kondo, Y., Hitomi, M., Barnett, G. H., Ishizaka, Y., Liu, J., Haqqi, T., Nishiyama, A., Villeponteau, B., Cowell, J. K., and Barna, B. P. Antisense telomerase treatment: induction of two distinct pathways, apoptosis and differentiation. *FASEB J.*, **12**: 801–811, 1998.
- Shammas, M. A., Simmons, C. G., Corey, D. R., and Reis, R. J. Telomerase inhibition by peptide nucleic acids reverses "immortality" of transformed human cells. *Oncogene*, **18**: 6191–6200, 1999.
- Izbicka, E., Wheelhouse, R. T., Raymond, E., Davidson, K. K., Lawrence, R. A., Sun, D., Windle, B. E., Hurley, L. H., and Von Hoff, D. D. Effects of cationic porphyrins as G-quadruplex interactive agents in human tumor cells. *Cancer Res.*, **59**: 639–644, 1999.
- Shammas, M. A., Xia, S. J., and Shmookler Reis, R. J. Induction of duplication reversion in human fibroblasts, by wild-type and mutated SV40 T antigen, covaries with the ability to induce host DNA synthesis. *Genetics*, **146**: 1417–1428, 1997.
- Xia, S. J., Shammas, M. A., and Shmookler Reis, R. J. Reduced telomere length in ataxia-telangiectasia fibroblasts. *Mutat Res.*, **364**: 1–11, 1996.
- Bechter, O. E., Eisterer, W., Pall, G., Hilbe, W., Kuhr, T., and Thaler, J. Telomere length and telomerase activity predict survival in patients with B cell chronic lymphocytic leukemia. *Cancer Res.*, **58**: 4918–4922, 1998.
- Ohashi, K., Tsutsumi, M., Kobitsu, K., Fukuda, T., Tsujiuchi, T., Okajima, E., Ko, S., Nakajima, Y., Nakano, H., and Konishi, Y. Shortened telomere length in hepatocellular carcinomas and corresponding background liver tissues of patients infected with hepatitis virus. *Jpn. J. Cancer Res.*, **87**: 419–422, 1996.
- Odagiri, E., Kanada, N., Jibiki, K., Demura, R., Aikawa, E., and Demura, H. Reduction of telomeric length and *c-erbB-2* gene amplification in human breast cancer, fibroadenoma, and gynecocoma. Relationship to histologic grade and clinical parameters. *Cancer*, **73**: 2978–2984, 1994.
- Sommerfeld, H. J., Meeker, A. K., Piatyszek, M. A., Bova, G. S., Shay, J. W., and Coffey, D. S. Telomerase activity: a prevalent marker of malignant human prostate tissue. *Cancer Res.*, **56**: 218–222, 1996.
- Grand, C. L., Han, H., Munoz, R. M., Weitman, S., Von Hoff, D. D., Hurley, L. H., and Bearss, D. J. The cationic porphyrin TMPyP4 down-regulates c-MYC and human telomerase reverse transcriptase expression and inhibits tumor growth *in vivo*. *Mol. Cancer Ther.*, **1**: 565–573, 2002.
- Shmookler Reis, R. J. and Shammas, M. A. DNA instability, telomeric recombination, and cell transformation. In: B. A. Gilchrist and V. A. Bohr (eds.), *The Role of DNA Damage and Repair in Cellular Aging*, in press, 2003.
- Shammas, M. A. and Shmookler Reis, R. J. Recombination and its roles in DNA repair, cellular immortalization and cancer. *Age*, **22**: 71–88, 1999.
- Counis, M. F. and Torriglia, A. DNases and apoptosis. *Biochem. Cell Biol.*, **78**: 405–414, 2000.

33. Boone, D. L. and Tsang, B. K. Caspase-3 in the rat ovary: localization and possible role in follicular atresia and luteal regression. *Biol. Reprod.*, **58**: 1533–1539, 1998.
34. Yakovlev, A. G., Wang, G., Stoica, B. A., Simbulan-Rosenthal, C. M., Yoshihara, K., and Smulson, M. E. Role of DNAS1L3 in Ca²⁺- and Mg²⁺-dependent cleavage of DNA into oligonucleosomal and high molecular mass fragments. *Nucleic Acids Res.*, **27**: 1999–2005, 1999.
35. Lauber, K., Appel, H. A., Schlosser, S. F., Gregor, M., Schulze-Osthoff, K., and Wesselborg, S. The adapter protein apoptotic protease-activating factor-1 (Apaf-1) is proteolytically processed during apoptosis. *J. Biol. Chem.* **276**: 29772–29781, 2001.
36. Chen, M. and Wang, J. Initiator caspases in apoptosis signaling pathways. *Apoptosis*, **7**: 313–319, 2002.
37. Inohara, N., Koseki, T., Hu, Y., Chen, S., and Nunez, G. CLARP, a death effector domain-containing protein interacts with caspase-8 and regulates apoptosis. *Proc. Natl. Acad. Sci. USA*, **94**: 10717–10722, 1997.
38. Chang, H. Y. and Yang, X. Proteases for cell suicide: functions and regulation of caspases. *Microbiol. Mol. Biol. Rev.*, **64**: 821–846, 2000.
39. Li, W., Maeda, Y., Ming, X., Cook, S., Chapin, J., Husar, W., and Dowling, P. Apoptotic death following Fas activation in human oligodendrocyte hybrid cultures. *J. Neurosci. Res.*, **69**: 189–196, 2002.
40. Shu, H. B., Halpin, D. R., and Goeddel, D. V. Casper is a FADD- and caspase-related inducer of apoptosis. *Immunity*, **6**: 751–763, 1997.
41. Xu, D., Wang, Q., Gruber, A., Bjorkholm, M., Chen, Z., Zaid, A., Selivanova, G., Peterson, C., Wiman, K. G., and Pisa, P. Downregulation of telomerase reverse transcriptase mRNA expression by wild type p53 in human tumor cells [In Process Citation]. *Oncogene*, **19**: 5123–5133, 2000.
42. Mata, J. E., Joshi, S. S., Palen, B., Pirruccello, S. J., Jackson, J. D., Elias, N., Page, T. J., Medlin, K. L., and Iversen, P. L. A hexameric phosphorothioate oligonucleotide telomerase inhibitor arrests growth of Burkitt's lymphoma cells *in vitro* and *in vivo*. *Toxicol. Appl. Pharmacol.*, **144**: 189–197, 1997.
43. Herbert, B., Pitts, A. E., Baker, S. I., Hamilton, S. E., Wright, W. E., Shay, J. W., and Corey, D. R. Inhibition of human telomerase in immortal human cells leads to progressive telomere shortening and cell death. *Proc. Natl. Acad. Sci. USA*, **96**: 14276–14281, 1999.